ACS OMEGA

Open Access

http://pubs.acs.org/journal/acsodf

Article

Onboard Large-Scale Isolation and Characterization of Three Reference DOM Materials from Siberian Arctic Shelf Marine Water

Anna N. Khreptugova,* Andrey I. Konstantinov, Tatiana A. Mikhnevich, Felipe Matsubara, Örjan Gustafsson,* Igor P. Semiletov, and Irina V. Perminova

Cite This: *ACS Omega* 2025, 10, 6406−6418

Read Online

ACCESS | Metrics & More | Article Recommendations | Supporting Information

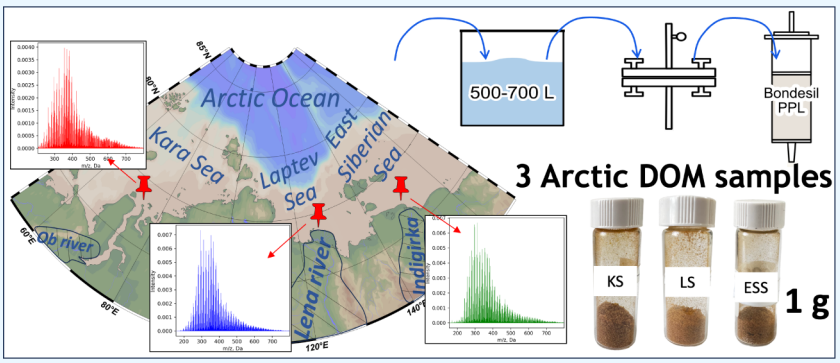

ABSTRACT: The Siberian Arctic Shelf is undergoing major climate change in the Northern Hemisphere, heavily impacted by a massive release of dissolved organic matter (DOM) due to degradation of permafrost as a consequence of global warming. This work is devoted to the isolation of large quantities of DOM from the Kara Sea, the Laptev Sea, and the East Siberian Sea, located from west to east along the Siberian Arctic Shelf. The goal was to isolate Arctic marine water reference DOM materials, addressing the gap in the set of available reference DOM materials. Large volumes of marine water (500−700 L) were collected from the three target seas and processed using a large-scale solid-phase extraction (SPE) setup aboard the research vessel "Academic Mstislav Keldysh" to establish a detailed molecular characterization of current Arctic DOM. The DOM was extracted using Bondesil PPL bulk sorbent at loading ratios ranging from 1:50 to 1:30 (on a DOC basis). The yield of DOM was 2 g from the Laptev Sea, 1.4 g from the Kara Sea, and 1.0 g from the East Siberian Sea. Detailed molecular characterization of the SPE DOM samples was conducted using elemental analysis, ^{13}C and ^{1}H NMR spectroscopy, FT-ICR mass spectrometry, and optical spectroscopy. All methods revealed that the DOM fromthe Kara Sea in West Siberia had a more oxidized and aromatic character compared to the DOM from the Laptev Sea and East Siberian Sea located on the East Siberian coast. The two latter DOM samples were less oxidized and richer in aliphatic structures. The Kara Sea sample was dominated by oxidized hydrolyzable tannins, while the Laptev Sea and East Siberian Sea samples were enriched with lignins and terpenoids. Fluorescence spectroscopy revealed a blue-shift in the DOM spectra from west to east, which may be linked to a decrease in humic-like fluorescence. Comparison with established terrestrial reference materials, such as Suwannee River fulvic acid and Suwannee River natural organic matter, demonstrates that the three Arctic DOM isolates provide a distinctive and valuable reference for studying marine DOM biogeochemistry.

INTRODUCTION

Arctic ecosystems are highly susceptible to global climate change and its consequences, as the region is now warming at four times the global average.[1] The majority of the region is occupied by permafrost, which consists of perennially frozen ground that is very rich in organic carbon (OC) (up to 10 wt %).[2] Global warming leads to substantial mobilization of dissolved organic matter (DOM) into the Siberian rivers and Arctic Ocean,[3−6] due to erosion of coastal and hinterland permafrost.[7−10] As a result, this massive release of permafrost OC impacts the molecular landscape of DOM in the Arctic Ocean.[11−14]

The Arctic Shelf functions as a natural receptor, which is essential for delineating large-scale footprint patterns of permafrost OC remobilization throughout the circum-Arctic region. It was recently demonstrated that nearly 80% of the terrestrial organic carbon exported around the circum-Arctic

Received: June 29, 2024
Revised: October 11, 2024
Accepted: October 18, 2024
Published: February 16, 2025

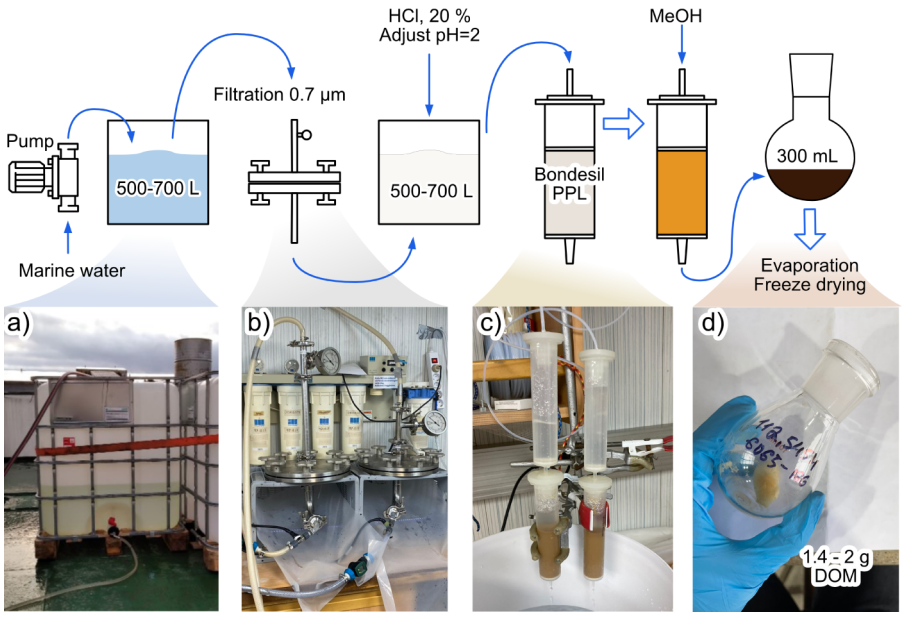

Figure 1. Principal scheme of the DOM isolation from large volume of seawater.

was directed to the Eurasian/Siberian side.[15] The East Siberian Arctic Shelf (ESAS), which includes the Laptev Sea (LS), the East Siberian Sea (ESS), and the Russian part of the Chukchi Sea (CS), is the world's largest continental shelf sea system. Its sediments are dominated by terrestrial organic carbon (terrOC), which accounts for 68% of the total OC.[15] The ESAS serves as a significant recipient of OC from both eroding coastal old permafrost deposits, which are the main source of terrOC released into the Laptev and East Siberian Seas.[16,17] It is also heavily impacted by the river basins of the Lena, Indigirka, and Kolyma, which are predominantly located in the continuous permafrost region. In contrast, the West Siberian Arctic Shelf (WSAS), specifically the Kara Sea (KS), represents the Ob-Irtysh River basin, which is situated in the discontinuous or sporadic permafrost zone.[18−20] An increase in the thawing of continuous permafrost was demonstrated to proceed along with an increase in the freshness of sedimentary OC and the lability of dissolved OC (DOC) along the Siberian Shelf.[21−24]

The Arctic is the most vulnerable region to global warming and requires continuous monitoring of ongoing climate processes. In recent years, there has been a growing number of land−ocean studies of the OC runoff in the Arctic Shelf, facilitating more active sampling and the establishment of a dense monitoring network. Due to the anticipated acceleration of permafrost degradation, there is an urgent need to establish a chemical DOM fingerprint to serve as a reference point over the coming years and decades, as the OM release and composition may change. For this purpose, bulk quantities of Arctic Shelf DOM reference samples are required.[25] Similar initiatives have recently been undertaken, including the isolation of coastal marine DOM reference material (TRM-0522) in gram quantities near Gothenburg, Sweden, for use in studies of marine DOM biogeochemistry.[26] Despite these efforts, there remains a pressing need for Arctic DOM reference materials.[26]

The aim of this study was to isolate gram quantities of DOM from surface seawater of the Arctic Siberian Shelf to be used as reference materials. To achieve this goal, three Arctic Shelf Seas−the Kara, Laptev, and East Siberian Seas, were selected due to the increasing contribution of permafrost runoff from West to East along the Siberian coastline. A large-scale onboard isolation of DOM was conducted in all three targeted seas using SPE with Bondesil PPL bulk sorbent. The isolated samples of SPE DOM were characterized using elemental analysis, Fourier Transform Ion Cyclotron Resonance Mass Spectrometry (FT-ICR MS), ^{1}H and ^{13}C NMR spectroscopy, and fluorescence and UV−vis spectroscopy.

RESULTS AND DISCUSSION

A recent evaluation comparing terrestrial OC release with circum-Arctic land carbon stocks indicates a predominant release from surface soils, accounting for approximately 59% in the KS, and around 50% in the LS and ESS.[15] The remaining terrestrial OC originates from Ice Complex Deposits (ESS and LS) and deep peat deposits (KS). Peat deposits contributed about 30% of the total fluvial release in the KS due to the Ob River discharge.[18−20] Consequently, one site was chosen near the outlet of the Ob Gulf (St. 6932) in the KS to presumably represent this large region with a strong "peat" signal (Figure 2). Two other sites were located in the regions strongly impacted by the Lena River (St. 6982) in the LS and by the coastal erosion plume near the Indigirka River mouth (St. 6969) in the western ESS.

The water was collected using a ship-based continuous seawater intake system (further detailed in S1), which is shown in Figure 1.

Large-Scale DOM SPE and Comparison of Collection Efficiencies with Different Setups and for Different Ocean Regimes. Three large-scale SPE isolations of DOM samples were conducted along the Siberian Arctic Shelf during the AMK-82 cruise at the sampling sites shown in Figure 2. The most western sampling site was located in the KS dominated by the Ob-Irtysh River plume (St. 6932), the central sampling site (St. 6980) was located in the LS dominated by the Lena River plume, and the most eastern site (St. 6969) was located in the ESS, near the erosion site on the Indigirka River. The corresponding river watersheds are shown

https://doi.org/10.1021/acsomega.4c06041
ACS Omega 2025, 10, 6406−6418

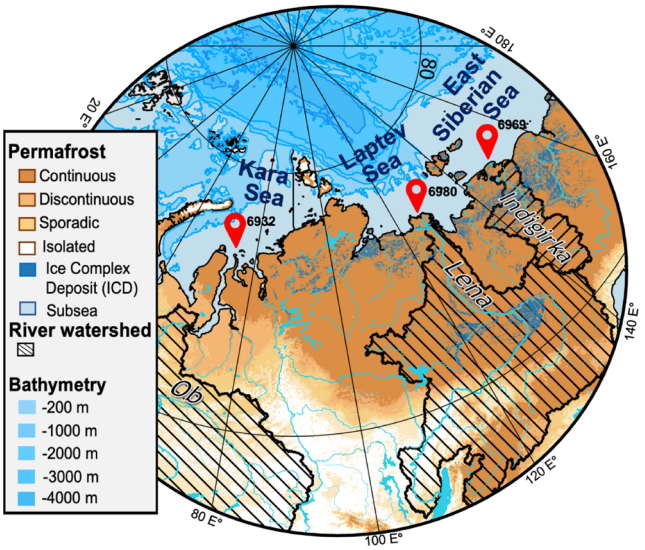

Figure 2. Siberian Arctic Shelf: red dots denote the sampling sites: St. 6932 is in the KS (within the Ob River plume), St. 6980 is in the LS (within the Lena River plume), and St. 6969 is in the ESS, near the erosion site on the Indigirka River.

with the shaded areas and the terrestrial permafrost including the Ice Complex Deposits[27] are plotted in accordance with Obu et al.[28] Coastline and rivers by Natural Earth Service were utilized as a background map, terrestrial permafrost zones are shown in accordance with Brown et al.,[29] the subsea permafrost in accordance with Overduin et al.[30]

It can be seen that three selected sampling regions were located along the Siberian Arctic Shelf in the west-east direction. Total volumes of the sampled water from each station accounted for 500 L for the KS and ESS samples, and 700 L for the LS samples. A total of ten DOM samples from the three stations were isolated using the SPE setup. The characteristics of large-scale extraction are represented in Table 1 (further details can be found in S2). In the marine waters of KS, LS, and ESS, DOC concentrations were measured at 4.1 mgOC·L^{-1}, 3.5 mgOC·L^{-1}, and 3.1 mgOC·L^{-1}, respectively. The DOC concentrations observed in all three investigated regions reflected typical seasonal levels characteristic for Arctic Shelf waters, which are influenced significantly by runoff from the Ob, Lena, and Indigirka Rivers.[31−34]

The KS recovery value was notably the highest (42 ± 6%, n = 3) as compared to those observed for the LS (31 ± 5%; n = 3) and ESS (28 ± 2%; n = 2) regions. We explain this variation in recovery values by the lowest loading of 34 mgOC/g of the SPE sorbent in the case of the KS, compared to the loading levels of 41 and 50 mgOC/g for the LS and ESS, respectively. Another explanation could be the molecular selectivity of the sorbent with regard to the components of DOM, which may also impact the recovery.[35] At the same time, the obtained recovery values are consistent with those reported for the Bond Elut PPL cartridges applied for marine water with high salinity.[35−38] So, in recent years, several advanced gram quantities of isolation were conducted. The work by Green et al.[39] demonstrated SPE with a usage of two sequential custom-built columns with 500 g of Bond Elut PPL each for extraction of DOM from 3000 L of ocean water. A large quantity of the sorbent was provided for its very low loading of 6 mg per g (0.006%), which enabled the extraction of 10.3 g of DOM from the combined surface and deep water samples. Felgate et al.[26] reported the isolation of 1.06 g of DOM reference material from 1500 L of coastal marine water using C18 sorbent with a sorbent mass 2398 g. In our study, we obtained grams of SPE DOM using much smaller amounts of Bondesil PPL sorbent. This could significantly reduce the costs of large-scale isolation of marine DOM, in particular, for onboard research vessel setups.

The elemental composition of the three DOM isolates from the Siberian Arctic Shelf is represented in Table 2 in comparison with the data on three aquatic IHSS reference materials, which could be found on the website of the IHSS.[40]

Among the three ESAS DOM samples, the most western (KS) sample was characterized with the lowest value of H/C ratio (1.15) and the lowest content of N (1.56). At the same time, two "eastern" DOM samples—LS and EES—were much more alike in H/C values (1.23 and 1.26, respectively) and had substantially higher content of nitrogen, in particular, ESS sample (1.81 versus 1.66 for the ES sample). Oxygen content was calculated as a difference between 100% of the total mass and the found mass of the CHNS elements. There was no substantial variation observed in the O/C ratio—it varied from 0.56 for the LS sample up to 0.59 for two other samples. In general, it can be concluded that two eastern samples were characterized with the enhanced contents of hydrogen, nitrogen, and sulfur as compared to the KS sample. When comparing the obtained data for the Arctic Shelf DOM with the two IHSS samples from the Suwannee River (SRNOM and SRFA), it is noteworthy that the H/C ratios are significantly lower (0.94 and 0.99), which are indicative of much more aromatic character of the Suwannee River NOM and FA, while the Arctic samples exhibit a more aliphatic character. A much closer H/C value of 1.23 was observed for PLFA, which is a sample isolated from the Antarctic lake and, therefore, has no lignin impact on the composition of DOM. However, PLFA has extremely high N content (6.51), which is very far from the highest value of 1.81 observed for the EES DOM. In general, it can be concluded that all three isolated ESAS DOM samples are characterized with predominantly aliphatic character and higher content of nitrogen and sulfur compared to the Suwannee River reference materials. They are very much alike, with subtle differences between the KS DOM versus two very similar LS and ESS DOM samples.

NMR Spectroscopy of the Arctic DOM. The ^{13}C and ^{1}H NMR data for all three sets of the Arctic DOM samples isolated in this study are given in Figure 3a,b, respectively. Table S2 represents the distribution of ^{13}C integral intensities. The carbon distribution was dominated by aliphatic structures

Table 1. Characteristics of Large-Scale Extraction for Three Arctic SPE Systems Used in this Study

Sampling region	Bondesil sorbent mass, g	DOC in marine water, mgOC·L^{-1}	Discharged volume, L	DOM yield, g	Loading mgOC per sorbent, g	Recovery of total DOC	DOC:sorbent ratio
KS	60	4.1	500	1.33	34	42 ± 6%	1:30
LS	60	3.5	700	2.07	41	34 ± 5%	1:24
ESS	30	3.1	500	1.02	50	28 ± 2%	1:20

https://doi.org/10.1021/acsomega.4c06041
ACS Omega 2025, 10, 6406−6418

Table 2. Elemental Composition of the SPE DOM Isolates Extracted in this Study and of the Three Reference Aquatic Materials of the IHSS

Sample	C, %	H, %	N, %	S, %	O,%	H/C	O/C	C/N
KS (n = 3)	52.2 ± 0.2	5.01 ± 0.06	1.56 ± 0.03	0.50 ± 0.10	40.73	1.15± 0.02	0.59	39.1± 0.6
LS (n = 3)	52.7 ± 0.1	5.42 ± 0.08	1.66 ± 0.07	0.81±0.05	39.41	1.23± 0.02	0.56	36.6± 0.4
ESS	51.5 ± 0.2	5.40 ± 0.06	1.81 ± 0.11	0.97±0.15	40.32	1.26± 0.01	0.59	33.2± 2.1
SRNOM (2R101N)[a]	50.7	3.97	1.27	1.78	42.28	0.94	0.63	46.5
SRFA (1S101F)[a]	52.44	4.31	0.72	0.44	42.09	0.99	0.60	87.4
PLFA (1R109F)[a]	52.47	5.39	6.51	3.03	32.60	1.23	0.47	9.4

[a]The elemental compositions of SRFA, SRNOM, and PLFA reference materials were obtained from IHSS website.[40]

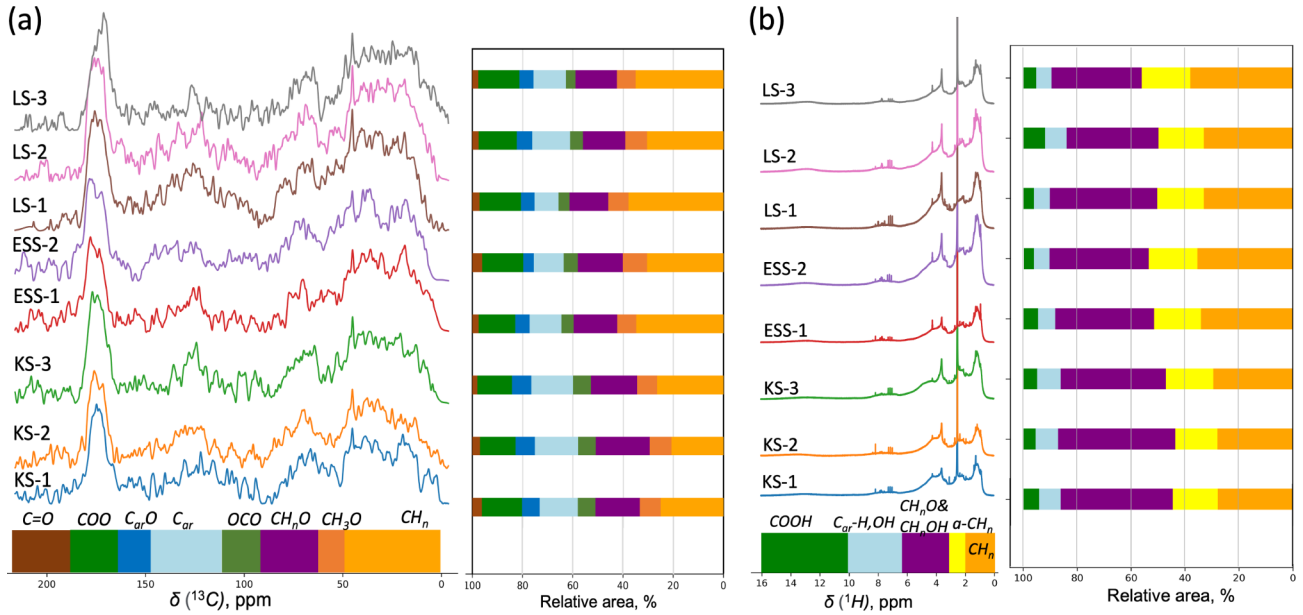

Figure 3. Distribution of integral intensities of C atoms (a) and H atoms (b) with different chemical environments in the DOM isolates from the KS (3 samples), LS (3 samples), and ESS (2 samples), as measured by ^{13}C and ^{1}H NMR spectroscopy.

reaching up to 65% of the total carbon in the LS and EES samples (Figure 3a).[41] These samples were also characterized with the highest contribution of nonsubstituted aliphatic structures (CH_n, δ < 50 ppm): it ranged from 30% to 37% of the total C, whereas the KS isolates contained from 20% to 27% of CH_n structures, and from 55% to 60% of the aliphatic C. The KS samples were characterized, on the contrary, by enhanced content of aromatic carbon reaching up to 25%, whereas the LS and ESS samples contained from 15% to 20% of aromatic structures. At the same time, the contents of carboxyls accounted for 16−18% and were very similar for the three sets of samples.

The lower levels of aromatic carbon (112−166 ppm) observed in the LS and EES samples align with the reduced concentrations of lignin and humic substances in the river runoff entering the ESAS during the autumn season.[23] The degree of aromaticity calculated as a ratio of aromatic to aliphatic carbon[42,43] accounted for (0.41 ± 0.02) for the KS and (0.29 ± 0.06) and (0.27 ± 0.02) for the LS and ESS samples, respectively. Very low values of aromaticity index are indicative of saturated character of Arctic DOM in general, and of the ESAS samples, in particular, which aligns well with the data of elemental analysis.

The found structural-group composition from the ^{13}C NMR data corroborate the reported data for DOM.[44,45] These data indicate that aliphatic structures are the most abundant component in the DOM of the ESAS regions, followed by carboxyls. The comparison with the PLFA, SRFA, and SRNOM reference materials, provided by IHSS,[40] revealed a significant distinction in the NMR spectra, particularly in the range of aliphatic structures (CH_n and CH_3O, 0−60 ppm). The KS DOM with a value of 33% exhibited a closer resemblance to SRFA and SRNOM (33% and 27%, respectively). The ESAS samples (42%) were the closest to the PLFA sample (61%) isolated from the Antarctic Lake. In terms of aromatics, (C_{ar}+$C_{ar}O$, 110−165 ppm), the lowest content was observed in the PLFA sample (12%), followed by ESAS samples (17%), and KS, SRFA, and SRNOM with 24%.

The ^{1}H NMR distribution demonstrated similar trends obtained for ^{13}C NMR (Figure 3b). Table S3 represents the distribution of ^{13}H integral intensities. The LS and ESS isolates contained up to 35% of protons of nonsubstituted aliphatic groups; the corresponding value for the KS DOM did not exceed 30%. The CH_n contribution exceeds substantially intensity of α-CH_n protons typically associated with CRAM (1.95−2.9 ppm). For the SRFA and SRNOM samples, the intensity of the CH_n protons is now comparable to that of the α-CH_n protons, each constituting 28% and 14% of the spectral intensity, respectively. The SRNOM sample and three KS samples exhibited an abundance of carbohydrates and peptides (up to 40%) signaling from 2.9 to 6.5 ppm.

The CH_n/α −CH_n index[46] had the highest value for the ESAS samples and accounted for (2.0 ± 0.1) and (1.9 ± 0.1) for the LS and ESS, respectively, which is in line with the

https://doi.org/10.1021/acsomega.4c06041
ACS Omega 2025, 10, 6406−6418

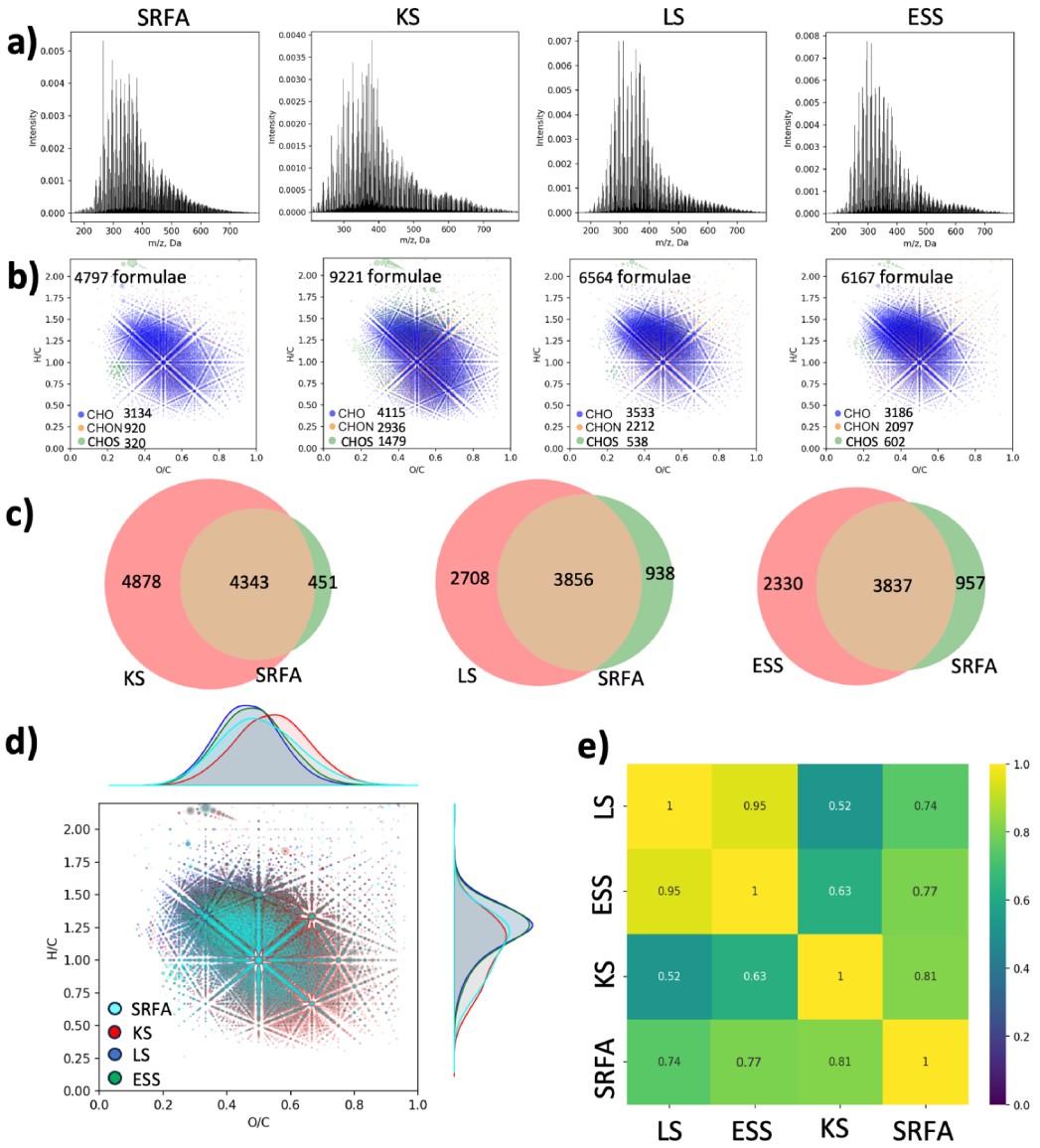

Figure 4. Comparison of the molecular compositions of the three sets of DOM isolates from the KS, LS, and ESS versus SRFA reference material: (a) typical mass-spectra of three SPE DOM isolates and SRFA (sum-normalized intensity), (b) typical VK diagrams for the DOM isolates and SRFA, (c) the Venn diagrams of intersections in molecular compositions for SPE DOM isolates versus SRFA, (d) all samples plotted in the same VK diagram with density axis: KS (highlighted in red), LS (highlighted in blue), ESS (highlighted in green), SRFA (highlighted in cyan), and (e) Tanimoto similarity index (T-score) calculated for each pair of the spectra used in this study. The color bar refers to the value of the T-score index.

highest contribution of least altered, long-chained methylenic structures in these samples.[44] The value of this index for the KS samples did not exceed (1.7 ± 0.1). The similar high values of this index were reported in our previous publication for the permafrost DOM released in the Kolyma River basin.[35] At the same time, the values for both SRFA and SRNOM samples did not exceed 1.1, which is indicative of the high contribution of α-CH_n structures present as a bridge between the aromatic ring and the COOH group, or other groups adjusted to aromatic rings. The deduced features are also in line with the Bond Elut PPL isolates of DOM from the Arctic Shelf region reported by other authors.[43,47−49]

The ^{1}H NMR spectral distributions of Arctic samples were aligned with those of the TRM-0522 sample,[26] as detailed in Table S4. The NMR profile of TRM-0522 closely mirrors that of SRFA, particularly in the low intensity of the aromatic (6.2−7.8 ppm) and peptide (4.1−4.8 ppm) regions. This similarity indicates a substantial transformation and advanced humification[46] of the in TRM-0522 material compared to the Arctic DOM isolates, which demonstrated less transformed structures.

The observed patterns suggest the higher contribution of least altered aliphatic components within the composition of Arctic DOM samples as compared to SRFA and SRNOM. This observation aligns well with the differences in the origin: the SRFA and SRNOM samples were extracted from the tropical "black river", which experienced active transformation and humification, whereas the Arctic DOM samples, dominated by low temperatures, inhibit the rapid decomposition of organic matter.

Molecular Composition of the SPE DOM Isolates as Measured by FT-ICR MS. The FT-ICR MS spectra of the SPE DOM samples from the three Arctic Seas isolated in this study revealed signals spanning the m/z range from 150 to 800

https://doi.org/10.1021/acsomega.4c06041
ACS Omega 2025, 10, 6406−6418

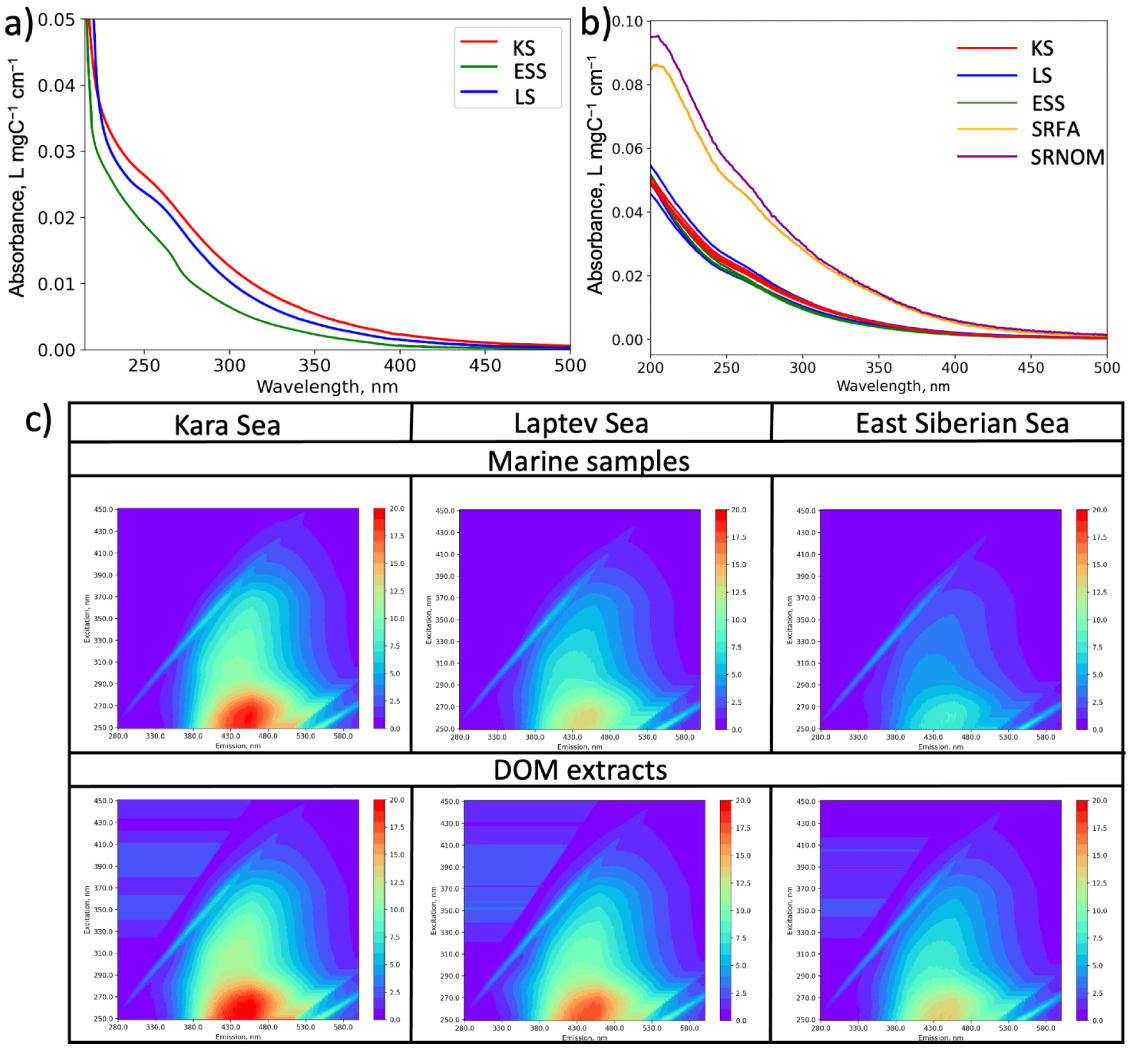

Figure 5. UV−vis spectra of initial marine water samples (a) and the corresponding Arctic DOM isolates (b) and the typical 2D spectra of the marine samples and three extracted DOM samples (c).

nm (Figure 4a). The corresponding van Krevelen (VK) diagrams typical of the obtained SPE DOM and of the reference SRFA material are presented in Figure 4b. The general characteristics of the FT-ICR MS data are summarized in Table S1. The number of assigned formulas was very similar for all DOM subsamples from the same station: (9453 ± 209) for the KS samples, (6265 ± 300) for the LS samples, and (6609 ± 625) for the EES samples. The SRFA sample exhibited 4797 formulas, primarily comprised of CHO formulas (65%), which is the dominant molecular composition[50] indicative of higher oxidation degree of the DOM materials.[51] The LS and ESS samples were characterized by a higher contribution of CHO, at (54.4 ± 0.5)% and (51.3 ± 0.5)%, respectively, compared to the KS value of (45.6 ± 1.1)%. Additionally, the number of N-containing formulas (CHON) was larger in the LS and ESS samples, at (32.7 ± 0.9)% and (33.5 ± 0.6)%, respectively, in contrast to the KS sample, which had a CHON content of (30.7 ± 0.9)%. The CHOS molecular formulas were twice as much in the KS samples, at (16.3 ± 0.4)%, compared to the ESAS DOM materials, which showed (8.2 ± 0.3)% and (9.3 ± 0.8)% in the LS and ESS, respectively. These trends in CHO, CHON, and CHOS formulas were commonly observed across the Arctic water DOM isolates.[26,52]

The VK formulas distributions observed both for the SRFA and the obtained SPE DOM samples was typical for aquatic DOM, with the majority of formulas falling within the region 1.0 < H/C < 1.5 and 0.3 < O/C < 0.7 (Figure 4b).[26,51] This area is typically occupied by the most recalcitrant DOM components, including "Island of Stability" molecules[53] and carboxyl-rich alicyclic molecules (CRAM) formulas.[54]

A pairwise comparison of the assigned molecular formulas of the three SPE isolates versus the SRFA reference material is represented in Figure 4c. The molecular compositions of the KS and SRFA are concentrated in almost the same area of the VK diagram; however, the KS sample is characterized by a higher abundance of unique molecular formulas (4878). Both the LS and ESS samples exhibit similar patterns in the distribution of the assigned molecular formulas compared to the SRFA sample, with approximately 40% of unique formulas in their molecular compositions.

Figure 4d represents a comparison of the VK diagrams of the SRFA reference material versus three SPE DOM isolates. In terms of distribution between H/C and O/C, the ESAS isolates (H/C 1.20 and O/C 0.46) were similar to the values of the coastal marine reference material TRM-0522 (1.28 and 0.46, respectively).[26] The KS sample (H/C 1.07 and O/C 0.52) was similar to that of the SRFA (1.02 and 0.50,

https://doi.org/10.1021/acsomega.4c06041
ACS Omega 2025, 10, 6406−6418

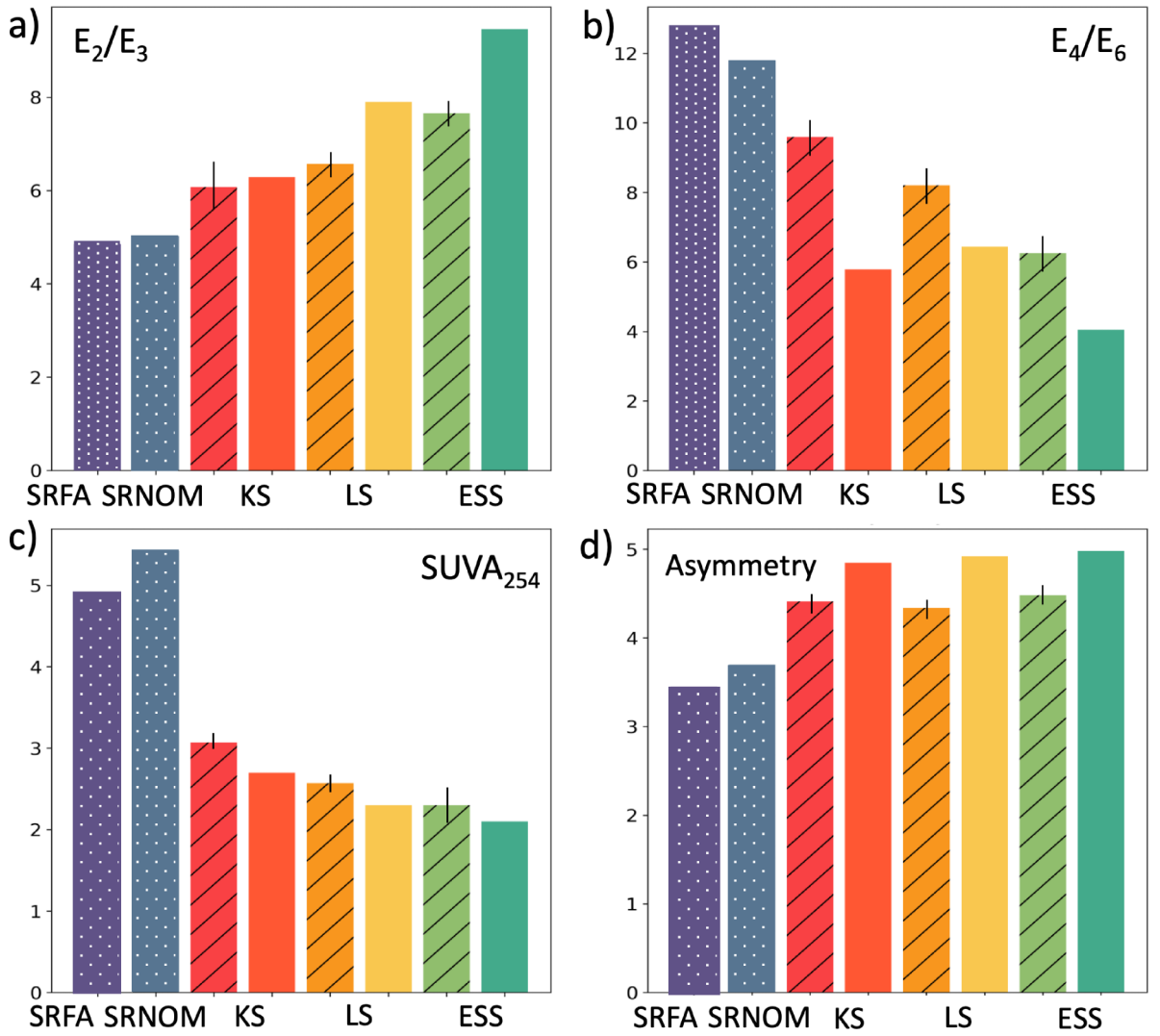

Figure 6. Optical parameters of the three Arctic DOM samples isolated in this study (shaded columns), three marine samples (plain columns) and two reference materials (SRFA and SRDOM): (a) E_2/E_3, (b) E_4/E_6, (c) $SUVA_{254}$ (L mgC^{-1} m^{-1}), and (d) fluorescence band shape asymmetry value.

respectively). The two ESAS isolates were characterized by a higher contribution of lignin-like[12] (1.0 < H/C < 1.4) and aliphatic[55] (1.5 < H/C) structures, along with a much lower oxidation degree (0.25 < O/C < 0.6) compared to the KS and SRFA samples, demonstrating overlap in the zone of unsaturated oxidized components—hydrolyzable tannins.[12] This can be indicative of the more processed− more humified character of the DOM in the KS, which is dominated by the inflow of the DOM from the Yenisei and Ob-Irtysh River systems, containing more aromatic and oxidized molecular structures.[31,56,57] In contrast, the DOM from the LS and ESS is more aliphatic due to an impact of the Lena, Indigirka and Kolyma Rivers, which drain areas with a high level of biolabile structures inherent in permafrost OM.[12,23,35,58]

To assess the similarities among the derived molecular compositions, Tanimoto similarity (T-score) indices were computed for each pair of mass spectra (Figure 4e). The T-score values between the three SPE DOM isolates and the SRFA reference sample ranged from 0.74 to 0.8, which is indicative of the close similarity in molecular composition. This suggests that the isolates shared 74% to 80% of the molecular formulas found in both the DOM SPE samples and the SRFA reference material. The highest similarity score with the SRFA samples was obtained for the KS sample (0.81), which aligns well with the prevalence of hydrolyzable tannins structures in these samples. At the same time, the highest similarity (0.95) was observed for the LS and ESS DOM isolates, which shared 95% of the identified formulas. This similarity may be attributed to the common sampling region in the ESAS.

Taken together, these data are indicative of the higher aromaticity, larger oxidation degree, and molecular weight of the KS DOM as compared to the DOM from ESAS (LS and ESS). The KS sample represents more humified transformed molecular structures of hydrolyzable tannins, whereas ESAS samples show abundance in low-oxidized biolabile aliphatic and lignin structures. The obtained FT ICR MS data are in good agreement with the above-discussed results of the elemental analysis and NMR spectroscopy.

UV−vis and Fluorescence of the Three Arctic DOM Materials and Marine Samples Obtained in this Study. The optical properties of Arctic DOM isolates and marine water samples were characterized using UV−vis and fluorescence spectroscopy (Figure 5). UV−vis spectra,

https://doi.org/10.1021/acsomega.4c06041
ACS Omega 2025, 10, 6406−6418

normalized to DOM concentration (mg/L) (Figure 5a,b), showed typical DOM absorbance.[34] The $SUVA_{254}$ values for marine water samples had the highest levels at the Kara Sea 2.50 L mgC^{-1} m^{-1}, and the lower levels at 2.07 L mgC^{-1} m^{-1} in the Laptev Sea, and 2.01 L mgC^{-1} m^{-1} in the East Siberian Sea. The $SUVA_{254}$ values observed are consistent with the range 2.0−3.2 L mg OC^{-1} m^{-1} typically found in the Arctic Shelf waters during the autumn season along transects extending from the deltas of the Lena and Ob Rivers to the continental slope.[59,60]

The typical excitation−emission matrixes (EEMs) of the three DOM isolates and for three marine water samples are shown in Figure 5c. The EEMs displayed certain similarities in peak positions for two sets of Arctic DOM samples. The 2D fluorescence spectra indicate the presence of terrigenous humic materials in the DOM samples.[61] Of particular interest is that the fluorescence band value[62] of the marine samples at 350 nm excitation wavelength exhibited a slight blue-shift (Figure 5b). This might be interpreted as the prevalence of protein-like fluorescence in those samples.[60,63] The same trends could be seen in the asymmetry parameter shown in Figure 6d.

The obtained spectral data were used to calculate optical indices, enabling a rapid evaluation of spatial variations in DOM characteristics. The $SUVA_{254}$ values (Figure 6c) showed a gradual decrease in DOM isolates from the KS (2.70 ± 0.15 L mgC^{-1} m^{-1}, $n = 3$) to LS (2.30 ± 0.09 L mgC^{-1} m^{-1}, $n = 3$) and ESS (2.10 ± 0.10 L mgC^{-1} m^{-1}, $n = 2$). The decrease in $SUVA_{254}$ values along the shelf suggests a decrease in the aromaticity of DOM isolates.[52] The $SUVA_{254}$ values showed significant differences among all three sets (paired t-test, $p < 0.01$) and were notably lower than the aromatics-dominated samples SRNOM (5.42 L mgC^{-1} m^{-1}) and SRFA (4.80 mgC^{-1} m^{-1}).[26] The $SUVA_{254}$ values for DOM extracts were significantly higher compared to those for marine water samples, supporting the hypothesis of molecular selectivity toward more hydrophobic and aromatic components in DOM when SPE sorbents are used for extraction.[35]

The E_2/E_3 values showed a significant difference (paired t-test, $p < 0.015$), indicating a higher proportion of aliphatic compounds and lower humification from the KS to LS and ESS DOM isolates (Figure 6a).[64] Pairwise comparisons of E_2/E_3 values between marine water and DOM extracts showed a significant reduction for the extracts, confirming a decrease in the aliphatic components in the reference samples. Moreover, the E_4/E_6 ratio (Figure 6b) gradually decreases from the KS to the ESAS samples (paired t-test, $p < 0.011$), suggesting a more humified nature of the samples, consistent with the findings from the ^{13}C NMR measurements, which revealed a decrease in aromatic structures. The fluorescence asymmetry values (Figure 6d) reveal the same trend, indicating a predominance of protein-like fluorescence in the marine water samples compared to the DOM extracts.[65] The low asymmetry values of SRDOM and SRFA samples suggest a high presence of humic-like fluorescence.

CONCLUSIONS

The large-scale SPE was designed for the isolation of DOM onboard the ship from large volumes of seawater (500−700 L). It allowed us to isolate gram quantities of DOM from remote regions of the Arctic Ocean, including the Kara Sea, Laptev Sea, and East Siberian Sea. The advantage of the developed Bondesil PPL method was its simplicity and low labor costs: it could be applied on-board without sophisticated instrumentation. The recovery of the Bondesil PPL sorbent was (42 ± 6)% ($n = 3$) in the case of the Kara Sea, (34 ± 5)% ($n = 3$) for the Laptev Sea sample, and (28 ± 2)% ($n = 2$) for the East Siberian Sea. The recovery differences may be attributed to the larger DOC loading of the SPE sorbent for the East Siberian Sea sample, which had a DOC/sorbent ratio of 1:20 (1 g of DOM per 30 g of the sorbent), and the Laptev Sea with a ratio of 1:24 (2 g per 60 g of the sorbent), compared to the Kara Sea sample, which had a ratio of 1:30 (1.4 g per 60 g of the sorbent). A comparison of the molecular characteristics and structural features of the DOM isolates obtained from the three different locations along the extended Eurasian Arctic Shelf revealed substantial differences: DOM from the Kara Sea was characterized by a higher content of aromatic structures—specifically hydrolyzable tannins—compared to that from the Laptev Sea and the East Siberian Sea DOM samples, which were dominated by more saturated lignin and terpenoid components. The optical measurements indicated a decrease in humic-like fluorescence along with an increase in the protein-like fluorescence in the KS sample versus the LS and ESS samples. The obtained data allowed us to speculate about a substantial gradient in the molecular properties of the DOM, from the oxidized state in the KS to a more reduced state in the LS and ESS regions.

The findings outlined in this paper establish three Arctic Shelf SPE DOM samples from the Kara Sea, Laptev Sea, and East Siberian Sea as valuable reference materials that adequately represent the coastal marine waters of the Arctic Siberian Shelf. These isolates are accessible to the broader scientific community; researchers interested in procuring samples should contact the corresponding author. The organic matter released into the Arctic Siberian Shelf may undergo significant changes in the near future due to global warming and anticipated acceleration of permafrost degradation. This makes the isolated Arctic Shelf SPE DOM materials valuable reference points for follow-up studies on molecular evolution of the DOM in this global climate-sensitive region.

EXPERIMENTAL SECTION

Site Description and Sampling Conditions. The large-scale setup for SPE was assembled aboard the research vessel "Academician Mstislav Keldysh" (AMK) during the AMK-82 expedition, which took place from 25/09/2020 to 02/11/2020. This expedition was also titled the International Siberian Shelf Study 2020 (ISSS-2020), which is part of a long-term collaborative program launched in early 2000s.[66] The large-scale SPE was performed in three widely separated systems of the Siberian Shelf including the KS region (°N 77°57′39″; °E 73°10′4″; St. 6932) with significant influence of the Ob and Yenisei Rivers; the LS region impacted by the Lena River (°N 73°59′25″; °E 130°4′9″; St. 6980); and the ESS region (°N 72°29′59″; °E 150°29′42″, St. 6969) with the combined influence of the Indigirka River and the Lena River (Figure 1). The regional map displayed in Figure 1 was generated using open-source QGIS software. The surface water at all locations had similar pH (7.9), whereas salinity differed from 21.1 to 23.3 PSU and temperature varied from 5.3 °C (KS) down to 1.4 and 1.3 °C (LS and ESS, respectively). Temperature and salinity in the surface water were continuously monitored using sensors mounted on the CTD Seabird 19+, which was deployed in the water column.

Water Sampling and SPE Setup. The sampling set up is shown in Figure 1. The HDPE 1000L tank filled with the

https://doi.org/10.1021/acsomega.4c06041
ACS Omega 2025, 10, 6406−6418

filtered seawater was connected to the 60 mL SPE cartridges (Agilent Technologies. Waldbronn. Germany) packed with 15 g of Bondesil PPL bulk sorbent (Agilent Technologies. Waldbronn. Germany) for achieving loading of about 0.1 g DOC per gram sorbent.[67] The loading level was based on the DOC content in the seawater samples.[68−70] The PVC pipe was split into two lines to make the SPE process parallel and more efficient.

For the KS marine water, a volume of 500 L was sampled with a DOC concentration of 4.1 mgOC·L^{-1} and discharged through the four columns packed with 15 g of Bondesil PPL sorbent. For the LS marine water, a volume of 700 L was sampled with a DOC concentration of 3.5 mgOC·L^{-1} and also discharged through four columns packed with 15 g of Bondesil PPL sorbent. For the ESS marine water, a volume of 500 L with a DOC concentration of 3.1 mgOC·L^{-1} was sampled and discharged through two columns packed with 15 g of Bondesil PPL sorbent. This lead to the highest DOC loading of these two columns.[31−34]

The SPE isolation was performed following Dittmar et al.[38] Four parallel cartridges filled with Bondesil PPL bulk sorbent were used at St. 6980 and 6932, while only two ones were applied for St. 6969. High-grade purity concentrated HCl (Chimmed, Russia) was used for acidification. The 500−700 L of acidified water sample was pumped through the self-packed cartridges at a constant rate of 100−120 mL·min^{-1} by means of a peristaltic pump (Fisherbrand, Germany). After passing half the volume of the seawater sample, the two parallel cartridges were replaced with two new cartridges to maintain a high recovery of the Bondesil PPL sorbent (further details can be found in S1).

DOM Isolation and DOC Measurements. DOM elution from the SPE columns was conducted with 300 mL of hypergrade methanol (for LC-MS LiChrosolv, Merck, Darmstadt, Germany)). The sample recovery was controlled by UV absorbance at 254 nm using a Carry 400 Probe spectrophotometer (Varian, Palo Alta, CA, USA) until a value of 0.1 was reached. The methanol eluent was collected into precombusted (450 °C, 4 h) round-bottom flasks and rotory evaporated until dryness. The residues were then dissolved in 5 mL of Milli-Q water and lyophilized using a freeze drier (Scientz-18ND Top Press multimanifolds, Scientz, Ningbo, Zhejiang, China). The dried DOM samples were transferred to precombusted glass vials and stored in the refrigerator at 4 °C in the dark.

DOC concentrations of the acidified seawater samples were measured using a total organic carbon analyzer (TOC-L_{CSN}, Shimadzu, Japan) in nonpurgeable organic carbon (NPOC) mode, with a sparging rate of 75 mL·min^{-1} for 8 min. DOC analysis was conducted in triplicates. An additional analysis was performed if the relative standard deviation (RSD) was >5%. The outliers were excluded (for more details, see S3).

CHNSO elemental analysis was performed on the isolated solid DOM samples using a 2400 Series II CHNS/O elemental analyzer (PerkinElmer, Waltham, MA, USA).

Fourier Transform Ion Cyclotron Resonance Mass Spectrometry. Ultrahigh-resolution mass spectra were acquired utilizing an electrospray ionization technique (ESI) on a Bruker solariX 15 T FT ICR mass spectrometer (Bruker Daltonics, Bremen, Germany) equipped with a 15 T superconducting magnet and an Apollo II source. The facilities are located at the Zelinski Institute of Organic Chemistry of the RAS (Moscow, Russia). The concentration of the DOM sample was adjusted to 50 mg/L by redissolving the dried matter in a solution of water and methanol in a 1:1 ratio. The spectra were acquired in accordance with Mueller et al.[71] (for more details see S4). SRFA samples provided by IHSS were used as reference material. The CHON formulas generated were validated by applying reasonable chemical constraints commonly observed for DOM (e.g., O/C ratio ≤1, 0.2 < H/C ratio ≤2.2, element counts [C ≤ 50, H ≤ 100, 0 < O ≤ 25, N ≤ 2, S≤ 1], and mass accuracy window <0.5 ppm). A table is then generated with all possible combinations of these elements, and the exact molecular weight was computed. Optionally, combinations that did not meet the specified conditions (O/C > 1, H/C > 2.2, DBE-O > 10) were excluded as unlikely for DOM. The obtained molecular assignments were used to calculate the H/C ratio and the O/C ratio. The relationship between these ratios was illustrated on van Krevelen diagrams, as described by Kim et al.[72]

Data processing was carried out using the open source NomSpectra software.[73] The Van Krevelen diagrams were quantitatively analyzed using a cell-partitioning algorithm outlined by Perminova.[12] These cells were categorized into seven primary chemotypes: condensed tannins, lignins, terpenoids, lipids, peptides, carbohydrates, and hydrolyzable tannins. The resulting occupational densities from the Van Krevelen diagram (for cells D1-D20 and chemotypes) were then utilized as quantitative indicators of the molecular composition. The values of double bond equivalent (DBE) were calculated[74,75] and used for further assessments in accordance with Koch et al.[76] Intensity distributions across all spectra were compared using the Tanimoto similarity score (T-score), as calculated in accordance with Schollée et al.;[77] the equation is represented in S4.

(^{1}H, ^{13}C) NMR Analysis. Quantitative ^{1}H and ^{13}C solution state NMR spectra were obtained with an Avance-400 spectrometer operating at 400 MHz proton frequency (Bruker BioSpin, Ettlingen, Germany). For ^{13}C NMR, DOM samples were dissolved in 99.9% D_2O at a concentration of 45 mg/mL, while for ^{1}H NMR, DMSO-d_6 was used at a concentration of 25 mg/mL. The conditions for quantitative acquisition were described in Hertkorn et al.[41] To exclude the Overhouser nuclear effect, the pulse technique INVGATE was implemented. The duration of relaxation time for ^{13}C NMR spectra acquisition was set to 8 s (0.2 s for the acquisition time and 7.8 s for the relaxation delay) to provide complete carbon nuclei relaxation.[41,78] The number of scans for 4500. Proton NMR spectra were acquired using a single 30° pulse, with a relaxation time of 5.1 s (4.1 s for the acquisition time and 1 s for the relaxation delay), and the number of scans was set to 64. The NMR spectra were obtained using a 5 mm broadband probe.

The ^{13}C NMR integrals were determined based on the following assignments: CH_n (0−47 ppm), CH_3O (47−58 ppm), CH_nO (57−92 ppm), OCO (92−112 ppm), C_{ar} (112−145 ppm), $C_{ar}O$ (145−166 ppm), COO (166−188 ppm), and C═O (188−220 ppm).[41] The ^{1}H spectral integration process involved utilizing the following chemical shift assignments: 0−1.95− ppm for protons of alkyl chains (CH_n−protons); 1.95−2.9− ppm for protons of carbon located in the α-position to the carboxyl group or to aromatic ring (CH_α−protons) (X-C_αH, X: COOH, COOR, C_{Ar}), which may also encompass resonances of amines and other functional groups; 2.9−6.5 ppm for protons of alkoxy and aliphatic hydroxyl groups, amines, and amides ($CH_nO(N)$, CH_n-O(N)H); 6.5−10.0 ppm for aromatic and phenolic protons (C_{Ar}H and C_{Ar}OH; where

https://doi.org/10.1021/acsomega.4c06041
ACS Omega 2025, 10, 6406−6418

C_{Ar} corresponds to aromatic carbon atoms); and 10.0−16.0 ppm for protons of carboxyl groups (COOH).[79]

Optical Measurements. Optical measurements for the isolated DOM samples and SRFA and SRNOM reference materials were conducted after the dry samples were redissolved in 0.01 M phosphate buffer at pH 6.8. UV−vis measurements for isolated DOM and initial marine water samples were performed with the use of a Carry 400 Probe spectrometer (Varian, Palo Alto, CA, USA). The specific UV absorbance ($SUVA_{254}$) for all isolated samples was calculated as a ratio of UV-absorbance at 254 nm normalized to the DOC (mg/L) concentration. The optical descriptors E_2/E_3 and E_4/E_6 were calculated as ratios of absorbances of 265 to 365 and 465 to 665, respectively. The calculated parameters were determined as described elsewhere.[46,80] Fluorescence spectra (1D) were acquired using a Fluorolog Tau-3 Lifetime System fluorimeter (Jobin-Yvon Horiba, Ltd., Japan) at λ_{ex} 350 nm and λ_{em} in the range from 300 to 700 nm.[62] The excitation and emission slit widths were 5 nm. The emission band asymmetry was calculated as the ratio of the integral intensities from 550 to 600 nm to those from 420 to 450 nm. This ratio serves as an indicator of the humification index.[81] The measurements were conducted in a quartz cuvette with a 1 cm optical path at ambient temperature (25 ± 2 °C). Optical indices and DOC concentrations were analyzed for significance, dataset standard deviation, and interindex comparison using *t*-tests with the python programming language.

■ ASSOCIATED CONTENT

Supporting Information

The Supporting Information is available free of charge at https://pubs.acs.org/doi/10.1021/acsomega.4c06041.

> Text for water sampling, characteristics of large-scale SPE system, DOC measurements, FT ICR MS formula assignment, comparison of general sorption characteristics of the sorbents; Table S1 for general FT-ICR MS characteristics of the DOM isolates; Table S2 and S3 for distribution of integral intensities of C and H atoms as measured by ^{13}C and ^{1}H NMR spectroscopy (PDF)

■ AUTHOR INFORMATION

Corresponding Authors

Anna N. Khreptugova − *Department of Chemistry, Lomonosov Moscow State University, Moscow 119991, Russia;* orcid.org/0000-0003-0521-9135; Email: khreprugova.anna@gmail.com

Örjan Gustafsson − *Department of Environmental Science, Stockholm University, Stockholm SE-106 91, Sweden; Bolin Centre for Climate Research, Stockholm University, Stockholm 114 19, Sweden*; Email: orjan.gustafsson@aces.su.se

Authors

Andrey I. Konstantinov − *Department of Chemistry, Lomonosov Moscow State University, Moscow 119991, Russia*

Tatiana A. Mikhnevich − *Department of Chemistry, Lomonosov Moscow State University, Moscow 119991, Russia*

Felipe Matsubara − *Department of Environmental Science, Stockholm University, Stockholm SE-106 91, Sweden; Bolin Centre for Climate Research, Stockholm University, Stockholm 114 19, Sweden*

Igor P. Semiletov − *Department of Chemistry, Lomonosov Moscow State University, Moscow 119991, Russia; Pacific Oceanological Institute, Far Eastern Branch of the Russian Academy of Sciences, Vladivostok 690041, Russia; National Tomsk State University, Tomsk 634050, Russia*

Irina V. Perminova − *Department of Chemistry, Lomonosov Moscow State University, Moscow 119991, Russia;* orcid.org/0000-0001-9084-7851

Complete contact information is available at: https://pubs.acs.org/10.1021/acsomega.4c06041

Author Contributions

Conceptualization, I.V.P., I.P.S., and Ö.G.; investigation, methodology, A.N.K. and F.M.; data analysis, A.N.K. and T.A.M.; investigation, A.N.K. and A.I.K.; writing—original draft preparation, A.N.K.; writing—review and editing, I.V.P., I.P.S., and Ö.G.; visualization, T.A.M. and A.N.K. All authors have read and agreed to the published version of the manuscript.

Notes

The authors declare no competing financial interest.

■ ACKNOWLEDGMENTS

The authors would like to acknowledge financial support of the Russian Science Foundation (grant no. 21-77-30001) in part of the DOM extraction and grant no. 21-73-20202 for the FTICR MS studies. The research of I.V.P. and A.I.K. was partially supported by the state budget funding 122040600057-3 (for NMR studies). The center of collective use of the Zelinsky IOC RAS is appreciated for availability of Solarix XR 15T (Bruker) FT-ICR MS mass spectrometer. Field work was also supported by the Ministry of Science and Higher Education (the Tomsk State Development Program "Priority −2030" and grant 0211-2021-0010 to POI). The research was further supported by funding from the Swedish Research Council (grant 2017-01601 to ÖG).

■ REFERENCES

(1) Rantanen, M.; Yu Karpechko, A.; Lipponen, A.; Nordling, K.; Hyvärinen, O.; Ruosteenoja, K.; Vihma, T.; Laaksonen, A. The Arctic Has Warmed Nearly Four Times Faster than the Globe since 1979. *Commun. Earth Environ.* **2022**, *3*, 168.

(2) Strauss, J.; Schirrmeister, L.; Mangelsdorf, K.; Eichhorn, L.; Wetterich, S.; Herzschuh, U. Organic-Matter Quality of Deep Permafrost Carbon-a Study from Arctic Siberia. *Biogeosciences* **2015**, *12*, 2227−2245.

(3) Wild, B.; Shakhova, N.; Dudarev, O.; Ruban, A.; Kosmach, D.; Tumskoy, V.; Tesi, T.; Grimm, H.; Nybom, I.; Matsubara, F.; et al. Organic Matter Composition and Greenhouse Gas Production of Thawing Subsea Permafrost in the Laptev Sea. *Nat. Commun.* **2022**, *13*, 5057.

(4) Savelieva, N. I.; Semiletov, I. P.; Vasilevskaya, L. N.; Pugach, S. P. A Climate Shift in Seasonal Values of Meteorological and Hydrological Parameters for Northeastern Asia. *Prog. Oceanogr.* **2000**, *47*, 279−297.

(5) Semiletov, I. P.; Savelieva, N. I.; Weller, G. E.; Pipko, I. I.; Pugach, S. P.; Gukov, A. Y.; Vasilevskaya, L. N. The Dispersion of Siberian River Flows into Coastal Waters: Meteorological, Hydrological and Hydrochemical Aspects *Freshwater Budget Of The Arctic Ocean*, 2000, 323−366.

(6) Frich, P.; Alexander, L. V.; Della-Marta, P.; Gleason, B.; Haylock, M.; Klein Tank, A. M. G.; Peterson, T. Observed Coherent Changes

in Climatic Extremes during the Second Half of the Twentieth Century. *Clim. Res.* **2002**, *19*, 193−212.
(7) Romanovskii, N. N.; Hubberten, H.-W.; Gavrilov, A. A. V.; Eliseeva, A. A.; Tipenko, A. G. S. Offshore Permafrost and Gas Hydrate Stability Zone on the Shelf of East Siberian Seas. *Geo-Mar. Lett.* **2005**, *25*, 167−182.
(8) Shakhova, N.; Semiletov, I.; Leifer, I.; Sergienko, V.; Salyuk, A.; Kosmach, D.; Chernykh, D.; Stubbs, C.; Nicolsky, D.; Tumskoy, V.; et al. Ebullition and Storm-Induced Methane Release from the East Siberian Arctic Shelf. *Nat. Geosci.* **2014**, *7*, 64.
(9) Shakhova, N.; Semiletov, I.; Gustafsson, O.; Sergienko, V.; Lobkovsky, L.; Dudarev, O.; Tumskoy, V.; Grigoriev, M.; Mazurov, A.; Salyuk, A.; et al. Current Rates and Mechanisms of Subsea Permafrost Degradation in the East Siberian Arctic Shelf. *Nat. Commun.* **2017**, *8*, 15872.
(10) Gavrilov, A. V.; Romanovskii, N. N.; Romanovsky, V. E.; Hubberten, H. W.; Tumskoy, V. E. Reconstruction of Ice Complex Remnants on the Eastern Siberian Arctic Shelf. *Permafr. Periglac. Process* **2003**, *14* (2), 187−198.
(11) Spencer, R. G. M.; Butler, K. D.; Aiken, G. R. Dissolved Organic Carbon and Chromophoric Dissolved Organic Matter Properties of Rivers in the USA. *J. Geophys. Res. Biogeosci.* **2012**, *117* (G3), 3001.
(12) Perminova, I. V. From Green Chemistry and Nature-like Technologies towards Ecoadaptive Chemistry and Technology. *Pure Appl. Chem.* **2019**, *91* (5), 851−864.
(13) Zhao, C.; Wang, Z.; Wang, C.; Li, X.; Wang, C. C. Photocatalytic Degradation of DOM in Urban Stormwater Runoff with TiO2 Nanoparticles under UV Light Irradiation: EEM-PARAFAC Analysis and Influence of Co-Existing Inorganic Ions. *Environ. Pollut.* **2018**, *243*, 177−188.
(14) McElmurry, S. P.; Long, D. T.; Voice, T. C. Stormwater Dissolved Organic Matter: Influence of Land Cover and Environmental Factors. *Environ. Sci. Technol.* **2014**, *48*, 45−53.
(15) Martens, J.; Wild, B.; Semiletov, I.; Dudarev, O. V.; Gustafsson, Ö. Circum-Arctic Release of Terrestrial Carbon Varies between Regions and Sources. *Nat. Commun.* **2022**, *13*, 1−10.
(16) Karlsson, E.; Gelting, J.; Tesi, T.; van Dongen, B.; Andersson, A.; Semiletov, I.; Charkin, A.; Dudarev, O.; Gustafsson, Ö. Different Sources and Degradation State of Dissolved, Particulate, and Sedimentary Organic Matter along the Eurasian Arctic Coastal Margin. *Global Biogeochem. Cycles* **2016**, *30* (6), 898−919.
(17) Vonk, J. E.; Sánchez-García, L.; Van Dongen, B. E.; Alling, V.; Kosmach, D.; Charkin, A.; Semiletov, I. P.; Dudarev, O. V.; Shakhova, N.; Roos, P.; Eglinton, T. I.; Andersson, A.; Gustafsson, O. ·. Activation of Old Carbon by Erosion of Coastal and Subsea Permafrost in Arctic Siberia. *Nature* **2012**, *489*, 137−140.
(18) Matsubara, F.; Wild, B.; Martens, J.; Andersson, A.; Wennström, R.; Bröder, L.; Dudarev, O. V.; Semiletov, I.; Gustafsson, O. Molecular-Multiproxy Assessment of Land-Derived Organic Matter Degradation Over Extensive Scales of the East Siberian Arctic Shelf Seas. *Global Biogeochem. Cycles* **2022**, *36* (12), No. e2022GB007428.
(19) Feng, X.; Vonk, J. E.; Van Dongen, B. E.; Gustafsson, Ö.; Semiletov, I. P.; Dudarev, O. V.; Wang, Z.; Montluçon, D. B.; Wacker, L.; Eglinton, T. I. Differential Mobilization of Terrestrial Carbon Pools in Eurasian Arctic River Basins. *Proc. Natl. Acad. Sci. U. S. A.* **2013**, *110* (35), 14168−14173.
(20) Gustafsson, O.; van Dongen, B. E.; Vonk, J. E.; Dudarev, O. V.; Semiletov, I. P. Widespread Release of Old Carbon across the Siberian Arctic Echoed by Its Large Rivers. *Biogeosciences* **2011**, *8*, 1737−1743.
(21) Mann, P. J.; Davydova, A.; Zimov, N.; Spencer, R. G. M.; Davydov, S.; Bulygina, E.; Zimov, S.; Holmes, R. M. Controls on the Composition and Lability of Dissolved Organic Matter in Siberia's Kolyma River Basin. *J. Geophys. Res.* **2012**, *117*, 1028.
(22) Mann, P. J.; Spencer, R. G. M.; Hernes, P. J.; Six, J.; Aiken, G. R.; Tank, S. E.; Mcclelland, J. W.; Butler, K. D.; Dyda, R. Y.; Holmes, R. M. Pan-Arctic Trends in Terrestrial Dissolved Organic Matter from Optical Measurements. *Front. Earth Sci.* **2016**, *4*, 25.
(23) Behnke, M. I.; McClelland, J. W.; Tank, S. E.; Kellerman, A. M.; Holmes, R. M.; Haghipour, N.; Eglinton, T. I.; Raymond, P. A.; Suslova, A.; Zhulidov, A. V.; et al. Pan-arctic Riverine Dissolved Organic Matter: Synchronous Molecular Stability, Shifting Sources and Subsidies. *Global Biogeochem. Cycles* **2021**, *35*, No. e2020GB006871.
(24) Rossel, P. E.; Bienhold, C.; Hehemann, L.; Dittmar, T.; Boetius, A. Molecular Composition of Dissolved Organic Matter in Sediment Porewater of the Arctic Deep-Sea Observatory HAUSGARTEN (Fram Strait). *Front. Mar. Sci.* **2020**, *7*, 7.
(25) Mopper, K.; Stubbins, A.; Ritchie, J. D.; Bialk, H. M.; Hatcher, P. G. Advanced Instrumental Approaches for Characterization of Marine Dissolved Organic Matter: Extraction Techniques, Mass Spectrometry, and Nuclear Magnetic Resonance Spectroscopy. *Chem. Rev.* **2007**, *107*, 419−442.
(26) Felgate, S. L.; Craig, A. J.; Moodie, L. W. K.; Hawkes, J. Characterization of a Newly Available Coastal Marine Dissolved Organic Matter Reference Material (TRM-0522). *Anal. Chem.* **2023**, *95* (16), 6559−6567.
(27) Strauss, J.; Laboor, S.; Schirrmeister, L.; Fedorov, A. N.; Fortier, D.; Froese, D.; Fuchs, M.; Günther, F.; Grigoriev, M.; Harden, J.; et al. Circum-Arctic Map of the Yedoma Permafrost Domain. *Front. Earth Sci.* **2021**, *9*, 758360.
(28) Obu, J.; Westermann, S.; Bartsch, A.; Berdnikov, N.; Christiansen, H. H.; Dashtseren, A.; Delaloye, R.; Elberling, B.; Etzelmüller, B.; Kholodov, A.; Khomutov, A.; Kääb, A.; Leibman, M. O.; Lewkowicz, A. G.; Panda, S. K.; Romanovsky, V.; Way, R. G.; Westergaard-Nielsen, A.; Wu, T.; Yamkhin, J.; Zou, D. Northern Hemisphere Permafrost Map Based on TTOP Modelling for 2000−2016 at 1km2 Scale. *Earth Sci. Rev.* **2019**, *193*, 299−316.
(29) Brown, J.; Ferrians, O. J.; Heginbottom, J. A.; Melnikov, E. S. *Circum-Arctic Map of Permafrost and Ground-Ice Conditions, Version 2*. NASA National Snow and Ice Data Center Distributed Active Archive Center. Colorado Boulder, USA. 1998, .
(30) Overduin, P. P.; Schneider von Deimling, T.; Miesner, F.; Grigoriev, M. N.; Ruppel, C.; Vasiliev, A.; Lantuit, H.; Juhls, B.; Westermann, S. Submarine Permafrost Map in the Arctic Modeled Using 1-D Transient Heat Flux (SuPerMAP). *J. Geophys. Res.: Oceans* **2019**, *124* (6), 3490−3507.
(31) Perminova, I. V.; Shirshin, E. A.; Zherebker, A.; Pipko, I. I.; Pugach, S. P.; Dudarev, O. V.; Nikolaev, E. N.; Grigoryev, A. S.; Shakhova, N.; Semiletov, I. P. Signatures of Molecular Unification and Progressive Oxidation Unfold in Dissolved Organic Matter of the Ob-Irtysh River System along Its Path to the Arctic Ocean. *Sci. Rep* **2019**, *9* (1), 19487.
(32) Dubinenkov, I.; Flerus, R.; Schmitt-Kopplin, P.; Kattner, G.; Koch, B. P. Origin-Specific Molecular Signatures of Dissolved Organic Matter in the Lena Delta. *Biogeochemistry* **2015**, *123* (1−2), 1−14.
(33) Semiletov, I. P.; Pipko, I. I.; Shakhova, N. E.; Dudarev, O. V.; Pugach, S. P.; Charkin, A. N.; Mcroy, C. P.; Kosmach, D.; Gustafsson, Ö. Carbon Transport by the Lena River from Its Headwaters to the Arctic Ocean, with Emphasis on Fluvial Input of Terrestrial Particulate Organic Carbon vs. Carbon Transport by Coastal Erosion. *Biogeosciences* **2011**, *8* (9), 2407−2426.
(34) Pugach, S. P.; Pipko, I. I.; Shakhova, N. E.; Shirshin, E. A.; Perminova, I. V.; Gustafsson, Ö.; Bondur, V. G.; Ruban, A. S.; Semiletov, I. P. Dissolved Organic Matter and Its Optical Characteristics in the Laptev and East Siberian Seas: Spatial Distribution and Interannual Variability (2003−2011). *Ocean Sci.* **2018**, *14*, 87−103.
(35) Perminova, I. V.; Dubinenkov, I. V.; Kononikhin, A. S.; Konstantinov, A. I.; Zherebker, A. Y.; Andzhushev, M. A.; Lebedev, V. A.; Bulygina, E.; Holmes, R. M.; Kostyukevich, Y. I.; et al. Molecular Mapping of Sorbent Selectivities with Respect to Isolation of Arctic Dissolved Organic Matter as Measured by Fourier Transform Mass Spectrometry. *Environ. Sci. Technol.* **2014**, *48* (13), 7461−7468.
(36) Minor, E. C.; Swenson, M. M.; Mattson, B. M.; Oyler, A. R. Structural Characterization of Dissolved Organic Matter: A Review of

https://doi.org/10.1021/acsomega.4c06041
ACS Omega 2025, 10, 6406−6418

Current Techniques for Isolation and Analysis. *Environ. Sci.: Processes Impacts* **2014**, *16* (9), 2064−2079.
(37) Swenson, M.; Oyler, A. R.; Minor, E. C. Rapid Solid Phase Extraction of Dissolved Organic Matter. *Limnol. Oceanogr.: Methods* **2014**, *12*, 713−728.
(38) Dittmar, T.; Koch, B.; Hertkorn, N.; Kattner, G. A Simple and Efficient Method for the Solid-Phase Extraction of Dissolved Organic Matter (SPE-DOM) from Seawater. *Limnol. Oceanogr.: Methods* **2008**, *6*, 230−235.
(39) Green, N. W.; Perdue, E. M.; Aiken, G. R.; Butler, K. D.; Chen, H.; Dittmar, T.; Niggemann, J.; Stubbins, A. An Intercomparison of Three Methods for the Large-Scale Isolation of Oceanic Dissolved Organic Matter. *Mar. Chem.* **2014**, *161*, 14−19.
(40) *IHSS, Elemental compositions and stable isotopic ratios of IHSS samples*. https://humic-substances.org/elemental-compositions-and-stable-isotopic-ratios-of-ihss-samples/. (Accessed 03 July 2024).
(41) Hertkorn, N.; Permin, A.; Perminova, I.; Kovalevskii, D.; Yudov, M.; Petrosyan, V.; Kettrup, A. Comparative Analysis of Partial Structures of a Peat Humic and Fulvic Acid Using One- and Two-Dimensional Nuclear Magnetic Resonance Spectroscopy. *J. Environ. Qual.* **2002**, *31*, 375−387.
(42) Perminova, I. V.; Grechishcheva, N. Y.; Petrosyan, V. S. Relationships between Structure and Binding Affinity of Humic Substances for Polycyclic Aromatic Hydrocarbons: Relevance of Molecular Descriptors. *Environ. Sci. Technol.* **1999**, *33*, 3781−3787.
(43) Ward, C. P.; Cory, R. M. Chemical Composition of Dissolved Organic Matter Draining Permafrost Soils. *Geochim. Cosmochim. Acta* **2015**, *167*, 63−79.
(44) Lam, B.; Baer, A.; Alaee, M.; Lefebvre, B.; Moser, A.; Williams, A.; Simpson, A. J. Major Structural Components in Freshwater Dissolved Organic Matter. *Environ. Sci. Technol.* **2007**, *41* (24), 8240−8247.
(45) Hertkorn, N.; Harir, M.; Koch, B. P.; Michalke, B.; Schmitt-Kopplin, P. High-Field NMR Spectroscopy and FTICR Mass Spectrometry: Powerful Discovery Tools for the Molecular Level Characterization of Marine Dissolved Organic Matter. *Biogeosciences* **2013**, *10* (3), 1583−1624.
(46) Perminova, I. V.; Shirshin, E. A.; Konstantinov, A. I.; Zherebker, A.; Lebedev, V. A.; Dubinenkov, I. V.; Kulikova, N. A.; Nikolaev, E. N.; Bulygina, ‖. E.; Holmes, R. M. The Structural Arrangement and Relative Abundance of Aliphatic Units May Effect Long-Wave Absorbance of Natural Organic Matter as Revealed by 1 H NMR Spectroscopy. *Environ. Sci. Technol.* **2018**, *52* (21), 12526−12537.
(47) Wang, J.-J.; Lafreniè, M. J.; Lamoureux, S. F.; Simpson, A. A.; Geíinas, Y.; Simpson, M. J. Differences in Riverine and Pond Water Dissolved Organic Matter Composition and Sources in Canadian High Arctic Watersheds Affected by Active Layer Detachments. *Environ. Sci. Technol.* **2018**, *52*, 1062−1071.
(48) Johnston, S. E.; Carey, J. C.; Kellerman, A.; Podgorski, D. C.; Gewirtzman, J.; Spencer, R. G. M. Controls on Riverine Dissolved Organic Matter Composition Across an Arctic-Boreal Latitudinal Gradient. *J. Geophys. Res. Biogeosci.* **2021**, *126* (9), No. e2020JG005988.
(49) Mutschlecner, A. E.; Guerard, J. J.; Jones, J. B.; Harms, T. K. Regional and Intra-Annual Stability of Dissolved Organic Matter Composition and Biolability in High-Latitude Alaskan Rivers. *Limnol. Oceanogr.* **2018**, *63* (4), 1605−1621.
(50) Herzsprung, P.; Hertkorn, N.; Von Tümpling, W.; Harir, M.; Friese, K.; Schmitt-Kopplin, P. Molecular Formula Assignment for Dissolved Organic Matter (DOM) Using High-Field FT-ICR-MS: Chemical Perspective and Validation of Sulphur-Rich Organic Components (CHOS) in Pit Lake Samples. *Anal. Bioanal. Chem.* **2016**, *408*, 2461−2469.
(51) D'Andrilli, J.; Foreman, C. M.; Marshall, A. G.; McKnight, D. M. Characterization of IHSS Pony Lake Fulvic Acid Dissolved Organic Matter by Electrospray Ionization Fourier Transform Ion Cyclotron Resonance Mass Spectrometry and Fluorescence Spectroscopy. *Org. Geochem.* **2013**, *65*, 19−28.
(52) Johnston, S. E.; Carey, J. C.; Kellerman, A.; Podgorski, D. C.; Gewirtzman, J.; Spencer, R. G. M. Controls on Riverine Dissolved Organic Matter Composition Across an Arctic-Boreal Latitudinal Gradient. *J. Geophys. Res. Biogeosci.* **2021**, *126*, 9.
(53) Lechtenfeld, O. J.; Kattner, G.; Flerus, R.; McCallister, S. L.; Schmitt-Kopplin, P.; Koch, B. P. Molecular Transformation and Degradation of Refractory Dissolved Organic Matter in the Atlantic and Southern Ocean. *Geochim. Cosmochim. Acta* **2014**, *126*, 321−337.
(54) Li, Y.; Harir, M.; Lucio, M.; Kanawati, B.; Smirnov, K.; Flerus, R.; Koch, B. P.; Schmitt-Kopplin, P.; Hertkorn, N. Proposed Guidelines for Solid Phase Extraction of Suwannee River Dissolved Organic Matter. *Anal. Chem.* **2016**, *88* (13), 6680−6688.
(55) Kellerman, A. M.; Dittmar, T.; Kothawala, D. N.; Tranvik, L. J. Chemodiversity of Dissolved Organic Matter in Lakes Driven by Climate and Hydrology. *Nat. Commun.* **2014**, *5*, 5.
(56) Frey, K. E.; McClelland, J. W.; Holmes, R. M.; Smith, L. G. Impacts of Climate Warming and Permafrost Thaw on the Riverine Transport of Nitrogen and Phosphorus to the Kara Sea. *J. Geophys. Res. Biogeosci.* **2007**, *112* (G4), 4−58.
(57) Polyak, L.; Levitan, M.; Khusid, T.; Merklin, L.; Mukhina, V. Variations in the Influence of Riverine Discharge on the Kara Sea during the Last Deglaciation and the Holocene. *Glob. Planet. Change.* **2002**, *32* (4), 291−309.
(58) Spencer, R. G. M.; Mann, P. J.; Dittmar, T.; Eglinton, T. I.; McIntyre, C.; Holmes, R. M.; Zimov, N.; Stubbins, A. Detecting the Signature of Permafrost Thaw in Arctic Rivers. *Geophys. Res. Lett.* **2015**, *42* (8), 2830−2835.
(59) Drozdova, A. N.; Nedospasov, A. A.; Lobus, N. V.; Patsaeva, S. V.; Shchuka, S. A. Cdom Optical Properties and Doc Content in the Largest Mixing Zones of the Siberian Shelf Seas. *Remote Sens.* **2021**, *13*, 1145.
(60) Drozdova, A. N.; Kravchishina, M. D.; Khundzhua, D. A.; Freidkin, M. P.; Patsaeva, S. V. Fluorescence Quantum Yield of CDOM in Coastal Zones of the Arctic Seas. *Int. J. Remote Sens.* **2018**, *39* (24), 9356−9379.
(61) Drozdova, A. N.; Krylov, I. N.; Nedospasov, A. A.; Arashkevich, E. G.; Labutin, T. A. Fluorescent Signatures of Autochthonous Dissolved Organic Matter Production in Siberian Shelf Seas. *Front. Mar. Sci.* **2022**, *9*, 9.
(62) Zherebker, A.; Shirshin, E.; Rubekina, A.; Kharybin, O.; Kononikhin, A.; Kulikova, N. A.; Zaitsev, K. V.; Roznyatovsky, V. A.; Grishin, Y. K.; Perminova, I. V.; Nikolaev, E. N. Optical Properties of Soil Dissolved Organic Matter Are Related to Acidic Functions of Its Components as Revealed by Fractionation, Selective Deuteromethylation, and Ultrahigh Resolution Mass Spectrometry. *Environ. Sci. Technol.* **2020**, *54*, 2667.
(63) Murphy, K. R.; Timko, S. A.; Gonsior, M.; Powers, L. C.; Wünsch, U. J.; Stedmon, C. A. Photochemistry Illuminates Ubiquitous Organic Matter Fluorescence Spectra. *Environ. Sci. Technol.* **2018**, *52* (19), 11243−11250.
(64) Stedmon, C. A.; Markager, S.; Kaas, H. Optical Properties and Signatures of Chromophoric Dissolved Organic Matter (CDOM) in Danish Coastal Waters. *Estuarine, Coastal Shelf Sci.* **2000**, *51* (2), 267−278.
(65) Walker, S. A.; Amon, R. M. W.; Stedmon, C. A. Variations in High-Latitude Riverine Fluorescent Dissolved Organic Matter: A Comparison of Large Arctic Rivers. *J. Geophys. Res. Biogeosci.* **2013**, *118*, 1689−1702.
(66) Semiletov, I.; Gustafsson, Ö. East Siberian Shelf Study Alleviates Scarcity of Observations. *EOS Trans. Am. Geophys. Union* **2009**, *90* (17), 145−146.
(67) Khreptugova, A. N.; Mikhnevich, T. A.; Molodykh, A. A.; Melnikova, S. V.; Konstantinov, A. I.; Rukhovich, G. D.; Volikov, A. B.; Perminova, I. V. Comparative Studies on Sorption Recovery and Molecular Selectivity of Bondesil PPL versus Bond Elut PPL Sorbents with Regard to Fulvic Acids. *Water* **2021**, *13* (24), 3553.
(68) Matsuoka, A.; Boss, E.; Babin, M.; Karp-Boss, L.; Hafez, M.; Chekalyuk, A.; Proctor, C. W.; Werdell, P. J.; Bricaud, A. Pan-Arctic Optical Characteristics of Colored Dissolved Organic Matter: Tracing

https://doi.org/10.1021/acsomega.4c06041
ACS Omega 2025, 10, 6406−6418

Dissolved Organic Carbon in Changing Arctic Waters Using Satellite Ocean Color Data. *Remote Sens. Environ.* **2017**, *200*, 89−101.
(69) Kaiser, K.; Canedo-Oropeza, M.; Mcmahon, R.; Amon, R. M. W. Origins and Transformations of Dissolved Organic Matter in Large Arctic Rivers. *Sci. Rep.* **2017**, *7* (1), 1−11.
(70) Paul, E. A. The Nature and Dynamics of Soil Organic Matter: Plant Inputs, Microbial Transformations, and Organic Matter Stabilization. *Soil Biol. Biochem.* **2019**, *98*, 109−126.
(71) Mueller, C.; Kremb, S.; Gonsior, M.; Brack-Werner, R.; Voolstra, C. R.; Schmitt-Kopplin, P. Advanced Identification of Global Bioactivity Hotspots via Screening of the Metabolic Fingerprint of Entire Ecosystems. *Sci. Rep.* **2020**, *10* (1), 1−13.
(72) Kim, S.; Kramer, R. W.; Hatcher, P. G. Graphical Method for Analysis of Ultrahigh-Resolution Broadband Mass Spectra of Natural Organic Matter, the Van Krevelen Diagram. *Anal. Chem.* **2003**, *75* (20), 5336−5344.
(73) Volikov, A.; Rukhovich, G.; Perminova, I. V. NOMspectra: An Open-Source Python Package for Processing High Resolution Mass Spectrometry Data on Natural Organic Matter. *J. Am. Soc. Mass Spectrom.* **2023**, *34*, 1524.
(74) Koch, B. P.; Witt, M. A.; Engbrodt, R.; Dittmar, T.; Kattner, G. Molecular Formulae of Marine and Terrigenous Dissolved Organic Matter Detected by Electrospray Ionization Fourier Transform Ion Cyclotron Resonance Mass Spectrometry. *Geochim. Cosmochim. Acta* **2005**, *69*, 3299−3308.
(75) Bae, E.; Yeo, I. J.; Jeong, B.; Shin, Y.; Shin, K.-H.; Kim, S. Study of Double Bond Equivalents and the Numbers of Carbon and Oxygen Atom Distribution of Dissolved Organic Matter with Negative-Mode FT-ICR MS. *Anal. Chem.* **2011**, *83*, 4193−4199.
(76) Koch, B. P.; Dittmar, T. From Mass to Structure: An Aromaticity Index for High-Resolution Mass Data of Natural Organic Matter. *Rapid Commun. Mass Spectrom.* **2006**, *20*, 926−932.
(77) Schollée, J. E.; Schymanski, E. L.; Stravs, M. A.; Gulde, R.; Thomaidis, N. S.; Hollender, J. Similarity of High-Resolution Tandem Mass Spectrometry Spectra of Structurally Related Micropollutants and Transformation Products. *J. Am. Soc. Mass Spectrom.* **2017**, *28* (12), 2692−2704.
(78) Kovalevskii, D. V.; Permin, A. B.; Perminova, I. V.; Petrosyan, V. S. Conditions for Acquiring Quantitative 13C NMR Spectra of Humic Substances. *Bull. Moscow Univ.* **2000**, *41* (2), 39−42.
(79) Dvorski, S. E. M.; Gonsior, M.; Hertkorn, N.; Uhl, J.; Müller, H.; Griebler, C.; Schmitt-Kopplin, P. Geochemistry of Dissolved Organic Matter in a Spatially Highly Resolved Groundwater Petroleum Hydrocarbon Plume Cross-Section. *Environ. Sci. Technol.* **2016**, *50* (11), 5536−5546.
(80) Arellano, A. R.; Bianchi, T. S.; Hutchings, J. A.; Shields, M. R.; Cui, X. Differential Effects of Solid-Phase Extraction Resins on the Measurement of Dissolved Lignin-Phenols and Organic Matter Composition in Natural Waters. *Limnol. Oceanogr. Methods* **2018**, *16* (1), 22−34.
(81) Zsolnay, A.; Baigar, E.; Jimenez, M.; Steinweg, B.; Saccomandi, F. Differentiating with Fluorescence Spectroscopy the Sources of Dissolved Organic Matter in Soils Subjected to Drying. *Chemosphere* **1999**, *38* (1), 45−50.

https://doi.org/10.1021/acsomega.4c06041
ACS Omega 2025, 10, 6406−6418